Three-Dimensional Metamaterials with an Ultrahigh Effective Refractive Index over a Broad Bandwidth

Jonghwa Shin (신종화),* Jung-Tsung Shen (沈榮聰),† and Shanhui Fan (范汕洄)‡

Ginzton Lab and Department of Electrical Engineering, Stanford University, Stanford, California 94305, USA

(Received 9 February 2008; revised manuscript received 28 December 2008; published 5 March 2009)

The authors introduce a general mechanism, based on electrostatic and magnetostatic considerations, for designing three-dimensional isotropic metamaterials that possess an enhanced refractive index over an extremely large frequency range. The mechanism allows nearly independent control of effective electric permittivity and magnetic permeability without the use of resonant elements.

DOI: 10.1103/PhysRevLett.102.093903 PACS numbers: 41.20.Jb, 42.70.Qs, 78.20.Ci, 78.67.Pt

One of the motivations for developing metamaterials is to achieve relative electric permittivity ε_r and magnetic permeability μ_r, in the ranges not readily accessible using naturally occurring materials [1]. In particular, creating an arbitrarily high refractive index ($n = \sqrt{\varepsilon_r \mu_r}$) is of interest for imaging and lithography, where the resolution scales inversely with the refractive index [2]. Moreover, increasing the refractive index over a large frequency range results in broadband slow light, which can be used to enhance the storage capacity of delay lines [3] as well as spectral sensitivity in interferometers [4].

In this Letter, we design three-dimensional metamaterials with an index of refraction that is arbitrarily high, over a broad frequency range extending down to near-zero frequencies. In contrast to our work, previous approaches to enhancing the refractive index utilized either electronic resonances in atoms [5] or electromagnetic resonances such as split-ring resonators [6,7]. These schemes are inherently narrowband and work only in the vicinity of a resonant frequency. Related to our work, it was discovered that the use of an array of subwavelength capacitors could lead to the frequency-independent and broadband enhancement of the relative electric permittivity ε_r [8–10]. However, all of the previously studied capacitive metamaterial structures exhibited strong diamagnetic behavior that suppressed the relative magnetic permeability μ_r in the low frequency regime [10–12]. Hence, in all previous systems, the capability of increasing the refractive index n was very limited.

Here, we propose a general mechanism to greatly enhance ε_r of a metamaterial without suppressing μ_r. The key idea is to generate a large electric dipole response, while simultaneously preventing the formation of large-area current loops. Below, we explain this idea using three crystal designs with progressive structural changes. All these structures consist of a cubic array of isolated perfect electric conductor (PEC) objects and have either an octahedral (O_h) or a pyritohedral (T_h) symmetry point group. Hence, their electromagnetic properties are isotropic [13,14], with ε_r and μ_r being scalars.

To begin with, we consider a simple cubic array structure of metal cubes [Fig. 1(a)]. For a structure with $b = 19a/20$, where a and b are the linear sizes of the unit cell and the metal cube, respectively, the transmission spectrum through a slab with a thickness of $10a$ is shown in the bottom panel of Fig. 1(a). These spectra were calculated using finite difference time domain (FDTD) schemes [15]. Accurate values of effective ε_r and μ_r can be extracted from such transmission spectra: the frequency spacing between the transmission peaks reveals the index of refraction, while the impedance can be found from the minimum value of the transmission coefficient. (Alternatively, we have also applied the s-parameter extraction method [16] to the transmission and reflection coefficients and obtained the same ε_r and μ_r.) The permittivity and permeability are found to be $\varepsilon_r = 20.0$ and $\mu_r = 0.098$, yielding $n = 1.4$. While this structure provides ε_r enhancement, it exhibits strong diamagnetism that suppresses μ_r. As a result, the structure demonstrates only a relatively modest increase in the refractive index, in agreement with Ref. [12].

To develop a physical intuition about this structure, we study its response to externally applied fields in the z-direction. For this structure, the opposing faces of the nearest-neighbor cubes form parallel-plate capacitors. Applying an electric field in the z-direction creates a large accumulation of surface charges due to such capacitors [top panel of Fig. 2(a)], resulting in a substantial dipole moment and large electric permittivity. Quantitatively, ε_r can be calculated with an area average, on the x-y plane, of the electric field in the air gap region, divided by a line average of electric field along the z-direction [6]. In the large cube limit (i.e., $b \approx a$), such a calculation yields $\varepsilon_r \approx \frac{a}{a-b}$.

When applying a quasistatic (but still time-varying) magnetic field in the z-direction, surface electric current is induced [middle panel of Fig. 2(a)] such that the magnetic field vanishes within the metal [bottom panel of Fig. 2(a)]. The magnetic moments generated by these surface currents align opposite to the applied magnetic field, making the structure diamagnetic. When the cubes

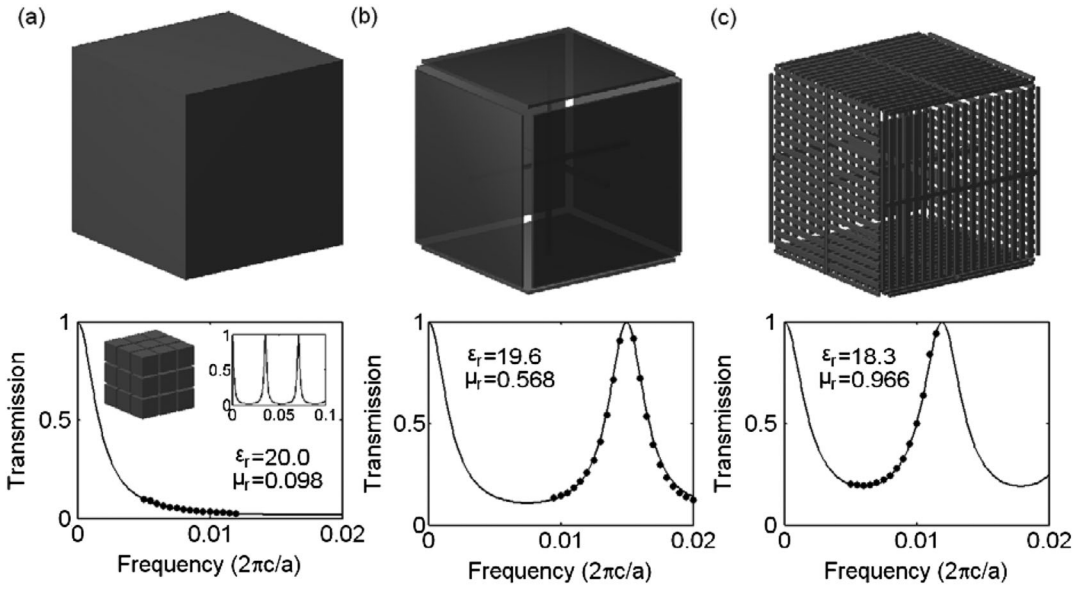

FIG. 1. Electromagnetic responses of metamaterials consisting of a cubic lattice of metallic objects. In all three structures, the outer dimension of the metallic objects is $19a/20$, where a is the lattice constant. In (a)–(c), the top panels show the object and the bottom panels are the corresponding transmission spectra through a slab of such metamaterial with a thickness of $10a$. The dots are from FDTD simulation and the lines are the response of a corresponding uniform medium with an effective ε and μ indicated. (a) Metallic cube. The left and right insets in the bottom panel show a structure with $3 \times 3 \times 3$ unit cells, and a transmission spectrum over broader frequency range, respectively. (b) A cube with connected metal plates. (c) Similar to (b), except that each plate now has slits.

are large, i.e., $b \approx a$, ignoring the small air gap normal to the field, one can approximate the permeability as $\mu_r = 1 - b^2/a^2 \approx 2(a-b)/a$, where b^2 and a^2 correspond to the cross-sectional areas of the cube and the unit cell, respectively. The analytic results of ε_r and μ_r agree with the numerical analysis. Such a strong diamagnetic response ($\mu_r \ll 1$), in fact, is present in all proposed metamaterial structures with a strong capacitive response [10–12]. All these systems therefore can not achieve broadband index enhancement.

A key observation, from the discussions above, is that ε_r and μ_r are controlled by different aspects of the structure. ε_r is determined by the induced charges on the surfaces normal to the electric field while μ_r is determined by the induced current loops flowing on the surfaces parallel to the magnetic field. The strength of magnetic dipole moment is proportional to the area subtended by the current loop.

Thus, to create a structure with an enhanced index, one should seek to suppress the diamagnetic response, by reducing the area subtended by the current loops, while maintaining a strong capacitive response. To do so, we first replace the cube with six metal plates connected by three orthogonal metal wires intersecting at the center of the unit cell [Fig. 1(b)]. To visualize its behavior, one can consider a simplified structure [Fig. 2(b)] with only two plates connected by a single wire along the z-direction, and apply external electric or magnetic fields along the z-direction. Comparing this simplified structure to the cube, we see that these two structures have an almost identical electric response since the surfaces normal to the electric field are identical [top panels, Figs. 2(a) and 2(b)]. On the other hand, the diamagnetic response is much weaker in the plate structure since most of the current loops now subtend much smaller areas [middle panels, Figs. 2(a) and 2(b)]. The magnetic fields therefore penetrate deeply into the regions behind the plate [bottom panel, Fig. 2(b)].

We now present the simulation results for the isotropic structure in Fig. 1(b) with six metal plates. The outer dimension of each metallic element is chosen to be the same as the cube, i.e., $b = 19a/20$. For this structure, ε_r and μ_r are found to be 19.6 and 0.568, respectively [from the spectrum in the bottom panel of Fig. 1(b)], yielding a refractive index n of 3.34. Indeed, while the permittivity of the structure is nearly identical to that of the cube structure, the permeability increases by more than fivefold.

Further suppression of the diamagnetic response can be accomplished by introducing air slits into the six plates [Fig. 1(c)]. Again, for visualization purposes, we first consider the simplified structure [Fig. 2(c)] with only two plates and a connecting wire along the z-direction, and apply the external fields along the z-direction [Fig. 2(c)]. The use of the slits results in further reduction in the area of the current loops in the plates [middle panel of Fig. 2(c)]. Consequently, the magnetic field now penetrates even deeper into the structure [bottom panel of Fig. 2(c)], signifying further suppression of the diamagnetic effect.

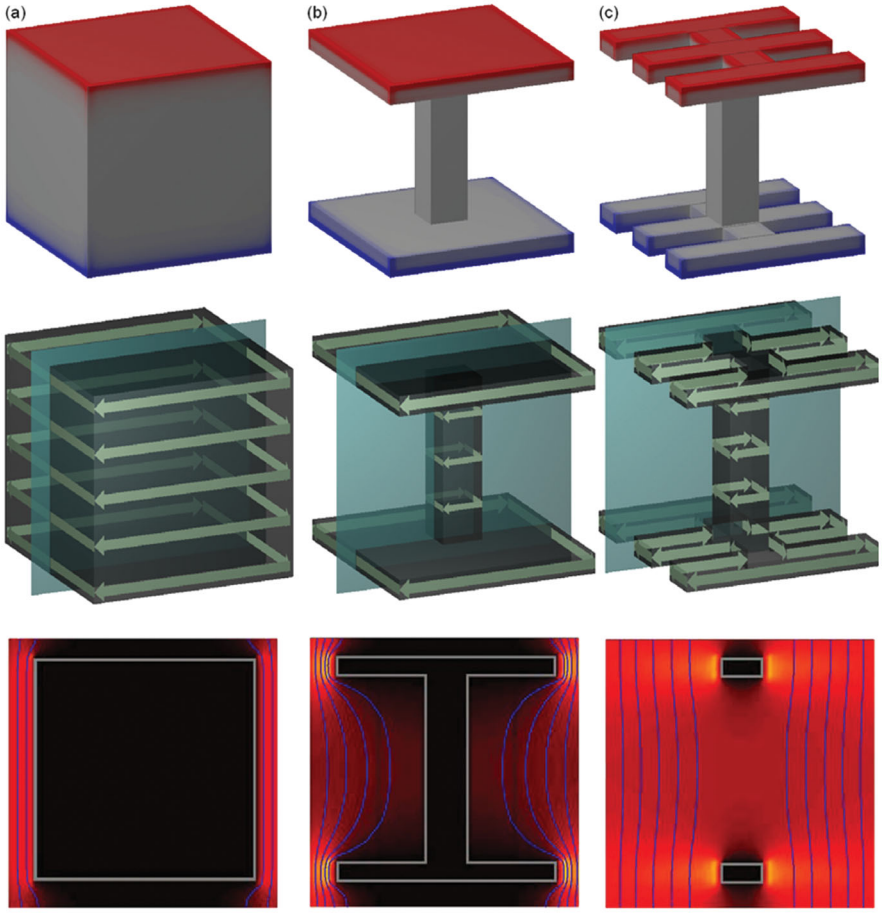

FIG. 2 (color). Electromagnetic response of metallic objects to externally applied electric and magnetic fields along the z-direction. The top panel in (a)–(c) shows the object, the colors indicate the charge distribution when the electric field is applied. The middle panel in (a)–(c) shows the current distribution when the magnetic field is applied. The bottom panels show the distribution and the direction of the total magnetic field on a slice as indicated in the middle panels. Gray lines indicate the boundaries of the metallic region. (a) A metallic cube. (b) Two metallic plates connected by a metal-wire. (c) Similar to (b), except that each plate now has slits.

On the other hand, the permittivity does not change significantly as long as the slits are narrow enough so that the electric fields are blocked from passing through. The charge distribution is now nonuniform on the metal plates, with the high concentration of charges near the edges of the slits compensating for those charges that were previously on the surface having been removed, and the total amount of surface charge in the top panel of Fig. 2(c) remains largely unchanged from Fig. 2(b). (This is the well-known fringe-field effect: the capacitance of a finite-size parallel-plate capacitor corresponds to an effective plate area that is larger than its physical size [17,18].)

We now consider the isotropic structure shown in Fig. 1(c). The FDTD simulations [bottom panel, Fig. 1(c)] show $\varepsilon_r = 18.3$ and $\mu_r = 0.966$, resulting in a refractive index of 4.2. Thus, the structure in Fig. 1(c) has approximately the same electric response as the cube structure in Fig. 1(a), but almost no magnetic response.

Starting from the class of structures in Fig. 1(c), one can further enhance the index by decreasing the air gap spacing between the metal plates of adjacent cells, and simultaneously reducing the thickness of plates, and the width and spacing of slits. (The number of slits in the plates increases as a result.) For demonstration, we chose the thickness of the plates, and the width and spacing between the slits all to be equal to the air gap spacing, (a-b), and compared different structures as we changed b. A semianalytic estimate based on field averaging predicts that $\varepsilon_r \propto \frac{a}{a-b}$ and $\mu_r \approx 1$, which agrees well with simulation results (Fig. 3). This simulation demonstrates the capability of creating an ultrahigh index metamaterial.

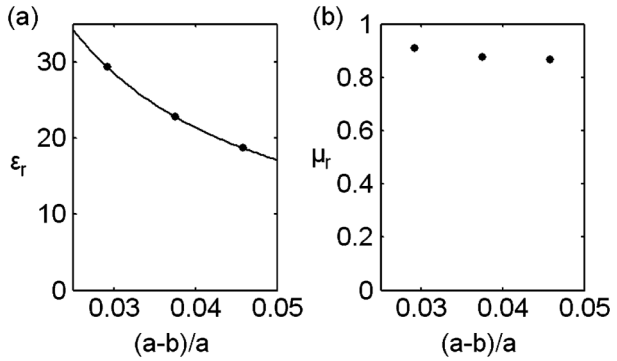

FIG. 3. Numerical results of (a) relative permittivity and (b) relative permeability as a function of $a - b$ in structures similar to Fig. 1(c), where b is the outer dimension of the metallic object, and a is the periodicity. The solid line is a theoretical prediction.

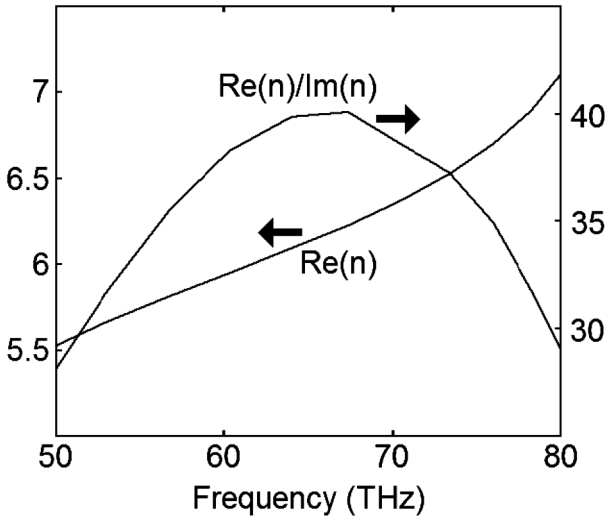

FIG. 4. Effective index of refraction when the loss of the metal (gold) is considered. The structure is the same as in Fig. 1(b). The real part of the index and the ratio of the real and imaginary parts (figure of merit) are shown.

All the discussions above assume perfect electric conductor inclusions surrounded by air. Replacing air with a dielectric material with an index of n_1 results in further enhancement of the effective index of the metamaterials by a factor of n_1. Our structure operates as an index enhancer: the metallic inclusions, when placed in a dielectric host, create a metamaterial with an effective index higher than the host itself. Therefore, this scheme in principle can achieve higher indices than any naturally existing dielectric material.

The predicted index-enhancement effect operates even when the lossy nature of real metals is considered, provided that the penetration depth into the metal is smaller than the thickness of the metal elements. As a demonstration, we simulated the connected-six-plate structure [Fig. 1(b)] assuming a 200 nm unit cell. The metal is assumed to be gold. In the wavelength range of 3–6 μm, we used a Drude model, which provides an accurate description of both the real and imaginary part of its permittivity [19]. The metallic inclusion is embedded in a dielectric host with an index of $n_1 = \sqrt{12} \approx 3.46$. The resulting metamaterial has an effective index between 5.5 and 7 in the $3 \sim 6$ micron wavelength range, clearly indicating the occurrence of the index enhancement effect over a broad bandwidth (Fig. 4). Moreover, the figure of merit (FOM), defined as $\mathrm{Re}(n)/\mathrm{Im}(n)$, is above 30 in most of this wavelength range. We note that such an FOM is commonly used in recent works on metamaterials [20–23] to characterize the effects of loss. An FOM larger than 10 is typically considered to be low loss to allow the important electromagnetic effects to be observed.

In conclusion, the index enhancement mechanisms here result only from the *shapes* of the metal objects and their relative size to the unit cell, and are independent of the absolute size of the elements, as long as the structural periodicity is far smaller than the wavelength. Consequently, in a very broad frequency range extending from microwave to midinfrared, one can achieve index enhancement using these structures.

This work is supported in part by ARO (Grant No. DAAD-19-03-1-0227), AFOSR (Grant No. FA9550-04-1-0437), and the DARPA Slow Light Program (Grant No. FA9550-04-0414). The simulations were carried out in the Pittsburgh Supercomputing Center through the support of the NSF LRAC.

*jshin@jshin.info
†jushen@gmail.com
‡shanhui@stanford.edu

[1] D. R. Smith, J. B. Pendry, and M. C. K. Wiltshire, Science **305**, 788 (2004).
[2] S. M. Mansfield and G. S. Kino, Appl. Phys. Lett. **57**, 2615 (1990).
[3] A. Karalis *et al.*, Phys. Rev. Lett. **95**, 063901 (2005).
[4] Z. Shi *et al.*, Phys. Rev. Lett. **99**, 240801 (2007).
[5] M. O. Scully, Phys. Rev. Lett. **67**, 1855 (1991).
[6] J. B. Pendry *et al.*, IEEE Trans. Microwave Theory Tech. **47**, 2075 (1999).
[7] C. Enkrich *et al.*, Phys. Rev. Lett. **95**, 203901 (2005).
[8] D. F. Sievenpiper *et al.*, Phys. Rev. Lett. **80**, 2829 (1998).
[9] J. T. Shen, P. B. Catrysse, and S. Fan, Phys. Rev. Lett. **94**, 197401 (2005).
[10] J. Shin, J. T. Shen, P. B. Catrysse, and S. Fan, IEEE J. Sel. Top. Quantum Electron. **12**, 1116 (2006).
[11] X. Hu *et al.*, Phys. Rev. Lett. **96**, 223901 (2006).
[12] B. Wood and J. B. Pendry, J. Phys. Condens. Matter **19**, 076208 (2007).
[13] V. M. Agranovich and V. L. Ginzburg, *Crystal Optics with Spatial Dispersion and Excitons* (Springer-Verlag, Berlin, 1984).
[14] P. Halevi and F. Perez-Rodriguez, Proc. SPIE Int. Soc. Opt. Eng. **6320**, 63200T (2006).
[15] S. Fan, P. R. Villeneuve, and J. D. Joannopoulos, Phys. Rev. B **54**, 11245 (1996).
[16] D. R. Smith, S. Schultz, P. Markos, and C. M. Soukoulis, Phys. Rev. B **65**, 195104 (2002).
[17] G. Kirchhoff, Monatsber. Dtsch. Akad. Wiss. Berlin, 144 (1877).
[18] G. J. Sloggett, N. G. Barton, and S. J. Spencer, J. Phys. A **19**, 2725 (1986).
[19] A. D. Rakić, A. B. Djurišić, J. M. Elazar, and M. L. Majewski, Appl. Opt. **37**, 5271 (1998).
[20] S. Zhang *et al.*, Phys. Rev. Lett. **95**, 137404 (2005).
[21] G. Dolling *et al.*, Opt. Lett. **30**, 3198 (2005).
[22] V. M. Shalaev *et al.*, Opt. Lett. **30**, 3356 (2005).
[23] J. Valentine *et al.*, Nature (London) **455**, 376 (2008).